Breeding for broad-spectrum disease resistance alters the maize leaf microbiome

Maggie R. Wagner[1,2*], Posy E. Busby[2], and Peter Balint-Kurti[1,3]

[1] Department of Entomology and Plant Pathology, North Carolina State University, Raleigh, North Carolina 27695, USA. [2] Department of Botany and Plant Pathology, Oregon State University, Corvallis, Oregon 97331, USA. [3] Plant Science Research Unit, Agricultural Research Service, United States Department of Agriculture

*Correspondence and requests for materials should be addressed to M.R.W. *Current address:* Department of Ecology and Evolutionary Biology and Kansas Biological Survey, University of Kansas, 1200 Sunnyside Avenue, Lawrence, KS, 66045, USA; maggie.r.wagner@ku.edu

Abstract:

Leaf-associated microbes can drastically affect disease severity, and host genotype can influence the diversity and composition of the leaf microbiome. However, these processes have not been studied and linked in the context of breeding for improved disease resistance. Here, we demonstrate that breeding for broad-spectrum disease resistance altered leaf microbiome composition in field-grown maize. Quantitative trait loci (QTL) conferring resistance to multiple fungal pathogens were introgressed into a disease-susceptible genetic background, and microbiome composition of the resulting near-isogenic lines was compared to that of the original susceptible parent line in five fields over two years. Introgression of disease-resistance alleles shifted the relative abundance of diverse fungal and bacterial taxa by up to 1000-fold in both 3-week-old and 7-week-old plants; however, these effects varied among fields and years. With few exceptions, host genotype effects were not any stronger in fields with high disease pressure than in uninfected fields, and microbiome succession over time was similar in heavily infected plants and uninfected plants. Overall, our results suggest that QTL for broad-spectrum disease resistance--or closely linked genes--have direct pleiotropic effects on the leaf microbiome in maize. Additional manipulative experiments will be needed to determine the consequences, if any, for plant health and disease resistance.

Introduction

Phyllosphere microbiomes—the communities of bacteria and fungi living on and in plant leaves—can profoundly affect the health of their plant hosts as well as the entire ecosystem (Lindow & Brandl 2003; Vorholt 2012; Laforest-Lapointe *et al.* 2017). Leaf-dwelling microbes can interfere with the exchange of gases and plant-derived volatiles at the leaf surface (Bringel & Couée 2015), alter patterns of herbivory (Clay 1990; Humphrey *et al.* 2014), participate in nitrogen cycling (Murty 1984; Papen *et al.* 2002; Fürnkranz *et al.* 2008), and influence drought resistance (Schardl *et al.* 2004; Rodriguez *et al.* 2009). Microbial symbionts are also noted for their role in disease resistance; manipulation of the phyllosphere microbiome can directly affect disease susceptibility in various plant species including tomato, poplar, wheat, and *Arabidopsis thaliana* (Massart *et al.* 2015; Busby *et al.* 2016; Ritpitakphong *et al.* 2016; Berg & Koskella 2018). Despite the importance of leaf microbiomes to plant health and productivity, little is known about whether they are affected by systematic changes in host genotype, such as those introduced by crop breeders. Existing studies of leaf microbiome heritability have compared distantly related genotypes to each other, or mutated genes to the wild type (Bodenhausen *et al.* 2014; Horton *et al.* 2014; Ritpitakphong *et al.* 2016; Wagner *et al.* 2016; Wallace *et al.* 2018). Here, we take a new approach by using germplasm from an active maize breeding experiment to compare maize leaf microbiome composition before and after the introgression of quantitative trait loci (QTL) for improved broad-spectrum disease resistance. Our study was designed to test whether systematic genetic changes commonly used in breeding programs have the potential to alter crop microbiomes, and to investigate the relationships between host genotype, disease resistance, and leaf-associated microbes.

The ecological, physiological, and molecular mechanisms by which the microbiome influences disease resistance appear to be complex and remain poorly understood. For instance, in *A. thaliana*, the foliar community did not directly inhibit the pathogen *Botrytis cinerea* but still conferred resistance via an unknown interaction with the plant host (Ritpitakphong *et al.* 2016). Inoculation with individual fungal endophytes was sufficient to substantially reduce symptoms of *Melampsora* rust infection in *Populus trichocarpa*, but other endophytes had no effect or even increased disease severity (Busby *et al.* 2016). And in tomato, the ability of the phyllosphere microbiome to improve resistance to *Pseudomonas syringae* depended on the nutrient status of the plant (Berg & Koskella 2018). These examples illustrate the need for further investigation of the links between pathogens, non-pathogenic members of the leaf microbiome, and their shared plant host.

One potential link between disease resistance and the microbiome is a shared sensitivity to the genotype of the host plant, which largely determines the plant phenotype. Host phenotype, in turn, determines the habitat available to both pathogenic and non-pathogenic microbes. Several studies have detected host genetic variation affecting features of the phyllosphere microbiome either among or within plant species (Sapkota *et al.* 2015; Wagner *et al.* 2016; Wallace *et al.* 2018), but most of the plant genes and traits that shape microbiome composition remain unknown. In laboratory settings, mutant studies in *A. thaliana* have shown that genes involved in cuticle synthesis also affect the composition of foliar bacterial communities (Bodenhausen *et al.* 2014; Ritpitakphong *et al.* 2016), and that salicylic acid

signaling and glucosinolate biosynthesis genes can alter root microbiome composition (Bressan *et al.* 2009; Lebeis *et al.* 2015). A genome-wide association study of field-grown *A. thaliana* revealed that genes affecting cell wall traits, defense-response pathways, and trichome development were overrepresented among the candidate genes at quantitative trait loci (QTL) affecting foliar microbiome composition (Horton *et al.* 2014). In poplar, down-regulation of a key enzyme in the lignin biosynthetic pathway caused dramatic changes in the composition of endophyte communities in leaves, stems, and roots (Beckers *et al.* 2016). In addition, evidence is mounting that the plant innate immune system is centrally involved in regulating microbial symbionts (Hacquard *et al.* 2017).

Some of the same plant traits implicated in microbiome variation have also been implicated in quantitative disease resistance (QDR), which is characterized by partial resistance to one or more pathogens (Poland *et al.* 2009; Niks *et al.* 2015; Beckers *et al.* 2016; Yang *et al.* 2017). For example, salicylic acid is a critical hormonal regulator of defense responses (Loake & Grant 2007); and while the leaf cuticle can be a physical barrier to pathogens and a reservoir for antimicrobial compounds, it also can be recognized and used by pathogens to stimulate invasion (Martin 1964; Bessire *et al.* 2007; Kachroo & Kachroo 2009; Serrano *et al.* 2014). QDR is a valuable target for crop improvement for several reasons. Compared to the nearly-complete immunity conferred by large-effect resistance (or “R”) genes, QDR is generally more difficult for pathogens to overcome via co-evolution (St Clair 2010). In addition, unlike the highly-specific R-genes, QDR genes can be effective against several pathogens, whether through pleiotropy or linkage (Wisser *et al.* 2011; Wiesner-Hanks & Nelson 2016; Yang *et al.* 2017). The resulting broad-spectrum protection, or multiple disease resistance (MDR), is desirable in situations where several pathogens are present or disease pressures are unpredictable.

By definition, MDR loci affect colonization success of multiple (pathogenic) microorganisms; therefore, we hypothesized that they might also influence the establishment of other microbiome members. MDR is usually a quantitative plant trait underlain by a large number of relatively small-effect genes, likely with diverse functions. A few MDR genes have been identified, such as the wheat ABC transporter gene *Lr34* that confers partial resistance to a wide range of biotrophic and hemibiotrophic pathogens (Krattinger *et al.* 2009; Wiesner-Hanks & Nelson 2016; Schnippenkoetter *et al.* 2017; Sucher *et al.* 2017). However, most of the mechanisms underlying MDR remain unknown. Despite this, systematic breeding methods such as controlled crosses and recurrent selection enable genetic improvement of this complex trait.

We used germplasm from an MDR breeding program to test whether MDR alleles have pleiotropic effects on the maize leaf microbiome. We compared the foliar microbiomes of improved and unimproved maize lines in several fields, at early- and late-season timepoints, both with and without pathogen infection. The resulting data enabled us to test several hypotheses. First, because our MDR lines were selected for resistance to three different fungal pathogens (Lopez-Zuniga et al. 2019), we hypothesized that the introgressed MDR alleles would have stronger effects on the fungal microbiome than the bacterial microbiome. Second, because these loci have known effects on disease resistance, we hypothesized that their effects on the microbiome would be stronger in environments with higher disease pressure (Figure 1). Finally, we hypothesized that disease establishment would disrupt patterns of microbiome succession over the growing season. Overall, our results provide partial support for each of

these hypotheses and suggest that breeding for broad-spectrum disease resistance has context-dependent side effects on the maize leaf microbiome.

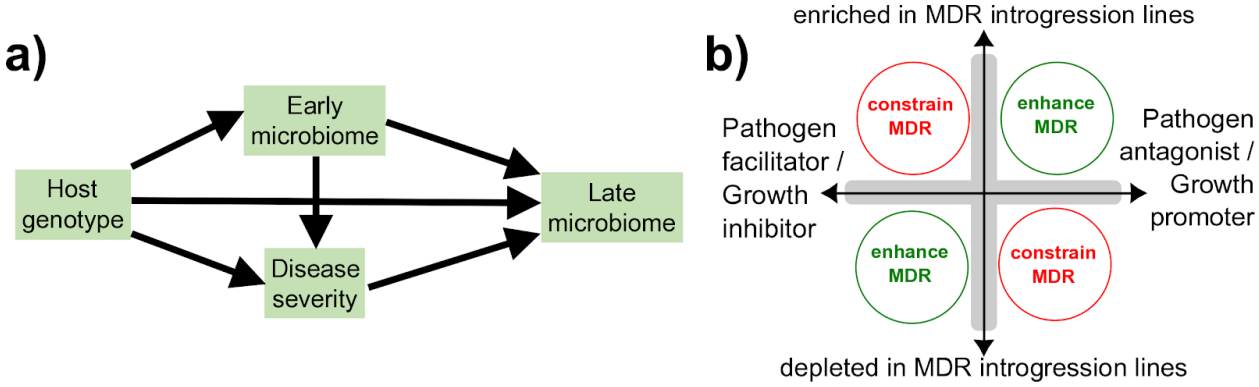

Figure 1 | Host-pathogen-microbiome relationships involve complex interactions among all community members. **(a)** In our simplified model, host genotype can affect the late-season microbiome both directly and through cascading effects via disease resistance; for this reason, we hypothesized that MDR alleles would exert stronger effects on the microbiome when disease pressure is higher. Furthermore, host genotype could affect disease severity both directly (via immune system and other traits that impact pathogen success) and indirectly (via traits that influence early microbiome assembly, which in turn interacts with the pathogen). **(b)** The repercussions of MDR-induced changes in a microbial symbiont's relative abundance (Figure 4) will depend on whether it has a positive effect, negative effect, or no effect on host health.

Materials and methods

Field experimental design

To directly test whether breeding for MDR affects the foliar microbiome, we compared microbiome composition of near-isogenic plants with and without introgressed chromosome segments that conferred MDR (Lopez-Zuniga *et al.* 2019). Briefly, two multiple disease resistant inbred lines (NC304 and Ki3) were crossed with H100, a line that is highly susceptible to multiple diseases. Using single seed descent, the resulting F_1 offspring were backcrossed three times to H100 and then self-fertilized for four generations. The resulting two populations of ~200 $BC_3F_{4:5}$ near-isogenic lines (NILs) were mostly genetically identical to the recurrent elite parent (H100) but retained small chromosome segments from the donor lines. On average, these introgressions covered 6.25% of the genome and were 78% homozygous (Figure 2; (Lopez-Zuniga *et al.* 2019). The NIL populations were assessed for resistance to three fungal pathogens: *Bipolaris maydis*, *Setosphaeria turcica*, and *Cercospora zeae-maydis*, the causative agents of the maize foliar diseases southern corn leaf blight, northern corn leaf blight, and grey leaf spot, respectively.

For this study, we selected eight NILs (four from each cross) that had high scores for resistance to all three pathogens. The relatively strong MDR phenotypes of these NILs likely reflect larger-than-average contributions from the MDR parent genome (roughly 10% per NIL, compared to the expected 6% based on the breeding design; (Lopez-Zuniga *et al.* 2019). Within each set of four NILs there was little overlap between introgressed regions, and cumulatively the NILs carried approximately 40% of each MDR parent genome (Figure S1). We planted these

eight NILs and their parent lines in a randomized design in multiple fields at the Central Crops Research Station in Clayton, NC (Table S1). Replicate plots were planted in two fields in 2016, and in four fields in 2017 (Figure 2c). Twenty kernels of each line were planted in each field, with the exception of the recurrent parent H100, which was planted at a replication of 30 kernels per field. Due to uneven germination, final sample sizes varied among replicates.

To reduce microbial inoculum from kernel surfaces, we soaked kernels in 3% hydrogen peroxide for two minutes and rinsed them in distilled water before planting. In each field, plants were randomly arranged in five to six adjacent rows of 40 to 50 plants each, spaced 12 inches apart. To reduce edge effects, we surrounded all experimental plots with two rows of border plants. All plots were maintained using standard agronomic conditions for rainfed maize. The four fields were all separated by <2 km and had similar soil types but different crop rotation histories (Figure 2b; Table S2).

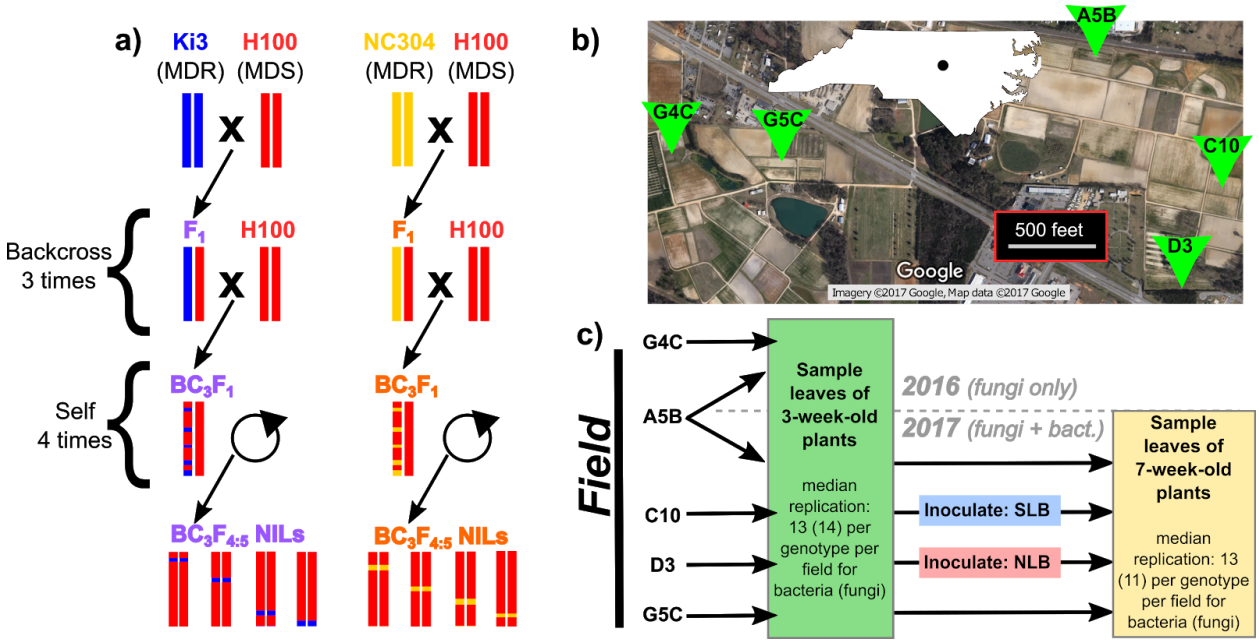

Figure 2 | Overview of experimental design. Panel **(a)** illustrates the crossing design used to generate the eight near-isogenic lines (NILs) used in this experiment, which were mostly genetically identical to their disease-susceptible parent line H100 but which had chromosome segments introgressed from a donor line (Ki3 or NC304) that conferred multiple disease resistance (MDR). Eight NILs were planted in randomized plots along with the three parent lines. Panel **(b)** shows the locations of the replicate plots within Central Crops Research Station, Clayton, NC, USA. Map data and imagery: Google. Panel **(c)** summarizes the sampling scheme for a total of six experimental replicate plots over two years. For the pilot experiment in 2016, only a single timepoint was sampled at two fields, and only fungi were quantified. In 2017, we quantified both bacteria and fungi; plants were sampled at two timepoints in four fields, two of which were inoculated with either southern leaf blight (SLB) or northern leaf blight (NLB).

Pathogen inoculation and disease scoring

In the 2017 experiment, we explored the effects of pathogen invasion on foliar microbiomes in maize by inoculating one-month-old plants in two of the four fields. Plants in field "C10" were inoculated with *C. heterostrophus*, plants in field "D3" received *S. turcica*, and plants

in the other two fields received no inoculation (Figure 2c). Inoculations were performed by incubating sterilized sorghum grains in pathogen cultures, and then dropping infected grains into the whorl of each plant (Sermons & Balint-Kurti 2018). Approximately 2 weeks after inoculation, we visually scored symptom severity of all inoculated individuals. Northern leaf blight symptoms were scored by estimating the percentage of each leaf damaged by lesions, and then averaging these scores for each plant. Southern leaf blight symptoms were scored for entire plants on a scale from 1 (complete leaf mortality) to 9 (asymptomatic) (Lopez-Zuniga *et al.* 2019). Disease scores were recorded using the Field Book application (Rife & Poland 2014).

Sample collection

In both 2016 and 2017, we collected leaf samples for microbiome quantification when plants were 3 weeks old. In 2017 only, we sampled leaves again when plants were 7 weeks old (i.e., 3 weeks after disease inoculations). For all sample collections, we used a standard hole punch to remove three discs evenly spaced from the base to the tip of a single leaf. For the early timepoint, we sampled the third leaf; in cases where the third leaf was too small or too damaged (<5% of plants), we sampled the second or fourth leaf instead. For the second timepoint we sampled the oldest leaf that was at least 50% green and was not touching the soil. Our rationale for this choice was that the microbiomes of older leaves were more likely to reflect host-driven processes than younger leaves, which were in earlier stages of microbiome assembly and more prone to stochastic influences (Maignien *et al.* 2014). Whenever possible, we selected green tissue and avoided lesions because we were primarily interested in direct genotype effects on non-pathogenic microbial symbionts, rather than microbiome responses driven by drastic differences in pathogen abundance (Figure S2). Leaf discs were collected into sterile tubes and stored on ice for the duration of sampling, then immediately transferred into -20°C for storage. Tools were rinsed in 70% ethanol between samples to reduce transfer of microbes among plants.

DNA extraction, library preparation, and sequencing

To remove loosely associated microbes from the leaf surface, we vortexed leaf discs in sterile water for 30 s on maximum speed and then shook them dry before freezing them at -80°C. Lyophilized leaf discs were randomly arranged into 96-well plates and ground to a fine powder using a Retsch MM301 mixer mill (1 minute at 25 Hz). Several wells were left empty as a negative control; to several others we added a mock microbial community as a positive control (ZymoBiomics Microbial Community Standard, Zymo Research, Irvine, CA, USA). We extracted DNA from all samples using the Synergy 2.0 Plant DNA Extraction Kit (OPS Diagnostics, Lebanon, NJ, USA) following the manufacturer's instructions, except that we doubled the length of the bead-beating step to increase microbial lysis. We eluted total DNA in 30 uL of 1x TE, pH 8.0.

We generated amplicon libraries separately for bacteria and fungi using a two-PCR-step approach. First, we amplified the barcoding genes 16S-V4 and ITS1 using the standard primer pairs 515f/806r for bacteria and ITS1f/ITS2 for fungi. Primers included upstream "frameshift"

stretches of 3 to 6 random nucleotides to increase library complexity and sequence quality, as well as a binding site for universal Illumina adaptors. Each 10-uL reaction included 0.4 uL of each primer (10 uM), 5 uL of 5Prime HotMasterMix (Quanta Bio, Beverly, MA, USA), 1.5 uL of template DNA, and 0.15 uL PNA PCR-blocker to reduce amplification of host plastid sequence (for bacterial libraries only; (Lundberg *et al.* 2013). We implemented an additional positive control at this stage: for several reactions, we used mock community DNA as the template (ZymoBiomics Microbial DNA Standard, Zymo Research). The PCR program for fungal libraries included an initial 2-minute denaturation at 95°C; 27 cycles of 20-second denaturation at 95°C / 20-second primer annealing at 50°C / 50-second extension at 72°C; and a final 10-minute extension step at 72°C. The PCR program for bacterial libraries was identical except that the primer annealing temperature was 52°C, and the primer annealing step was preceded by a 5-second PNA annealing step at 78°C. The resulting PCR products were cleaned by adding 7 uL of magnetic SPRI bead solution, washing magnet-bound DNA twice with 70% ethanol, and eluting in 10 uL ultrapure water.

The second PCR step added dual-indexed universal Illumina adaptors. The forward and reverse primers consisted of (from 5' to 3') the P5 or P7 adaptor sequence (respectively), a unique 8-bp index, and the binding site to enable annealing to amplicon sequences. PCR conditions were identical to those from the first step except that 1 uL of the first-step PCR product was used as the template DNA. We visualized the resulting libraries on a 1.5% agarose gel and then pooled 1 uL from each reaction to create separate pools for fungi and bacteria. We purified these pools by adding magnetic bead solution at a ratio of 0.8:1 (v/v), washing twice with 70% ethanol, and eluting DNA from the beads in ultrapure water. We then combined aliquots of the fungal and bacterial pools at equimolar concentrations.

The final combined pool derived from the 2017 samples was sequenced at 1,344-plex on an Illumina HiSeq2500 machine in Rapid Run mode (250 bp paired-end reads). Because this first sequencing run yielded ample ITS sequence but low coverage of 16S amplicons, we sequenced the 16S amplicon pool again on the HiSeq platform and on the Illumina MiSeq using V2 chemistry (250 bp paired-end reads) along with the smaller pool of ITS amplicons from the 2016 samples. All sequencing was performed by the North Carolina State University Genomic Sciences Laboratory (Raleigh, NC, USA).

Sequence processing and quality filtering

After trimming primers from raw, demultiplexed FASTQ files using CUTADAPT v1.12 (Martin 2011), we processed amplicon sequences using DADA2 v1.10.1 (Callahan *et al.* 2016). First, trimmed reads were quality-filtered. We required the forward and reverse 16S reads to have a maximum of 2 expected errors and no ambiguous bases, then truncated them at 220bp and 160 bp, respectively to remove low-quality sequence from 3' ends. We required the forward and reverse ITS reads to have a maximum of 1 and 2 expected errors (respectively) and no ambiguous bases but did not truncate reads to a fixed length. Error rates were inferred from $3x10^6$ reads; this was done separately for the ITS data and 16S data, and separately for each independent sequencing run. Quality-filtered reads were then de-replicated, de-noised, and merged to generate tables of amplicon sequence variants (ASVs). At this point we merged the

bacterial ASV tables from the three 16S sequencing runs with each other, and also merged the fungal ASV tables from 2016 and 2017, which had been sequenced separately. After removing chimeric ASVs, we assigned taxonomy using the RDP Classifier (Wang *et al.* 2007) trained on the RDP (v.16) training set for 16S sequences (Cole *et al.* 2014) and the UNITE database for ITS sequences (Kõljalg *et al.* 2005).

We discarded ASVs without taxonomic assignment at the kingdom level and ASVs that were assigned to chloroplasts or mitochondria ("non-usable reads"). We used the mock community positive controls to determine a within-sample relative abundance threshold that removed most contaminant ASVs while retaining as much of the data as possible. This threshold (0.091% for bacteria, 0.221% for fungi) was then applied to all non-control samples (Brown 2019). We then removed "non-reproducible" ASVs that were not observed at least 25 times in at least 5 samples (Lundberg *et al.* 2012). Together, these filtering steps reduced the final dataset to 1,502 bacterial ASVs while retaining 97.9% of the data. For fungi, the final dataset retained 548 ASVs and 93.8% of the original sequences. Finally, we excluded low-coverage samples from analysis (i.e., those with <500 usable reads). The number of reads remaining after all filtering steps was saved as the "sampling effort" for each sample; this variable was normalized and centered for use as a covariate in downstream analyses where appropriate.

Data analysis

We used R version 3.3.2 for all data analysis, especially the packages phyloseq, tidyr, lme4, DESeq2, vegan, and lmerTest (McMurdie & Holmes 2013; Love *et al.* 2014; Bates *et al.* 2015; Kuznetsova *et al.* 2017). When applicable, we used the Benjamini-Hochberg false discovery rate (Benjamini & Hochberg 1995) to adjust *P*-values from multiple comparisons. All analyses were performed in parallel for fungi and for bacteria. Original R code and raw data will be made freely available in a Dryad repository upon publication; raw reads will be deposited into the NCBI Sequence Read Archive.

Alpha diversity was characterized for each sample using the Shannon and abundance-based coverage estimator (ACE) metrics, which estimate community evenness and richness, respectively (Hughes *et al.* 2001). This was done prior to thresholding and removal of rare ASVs. For analyses conducted at higher taxonomic levels, we consolidated ASVs into their respective genera, families, orders, classes, or phyla using the function "Phyloseq::tax_glom" (McMurdie & Holmes 2013). For analyses that required normalization (*e.g.*, ordination) we applied the variance-stabilizing transformation from the "DESeq2" package (Love *et al.* 2014; McMurdie & Holmes 2014). Bray-Curtis dissimilarity of transformed count data was used to quantify community composition. Beta dispersion of groups of samples was calculated using the function "vegan::betadisper" (Oksanen *et al.* 2018). When modeling the relative abundances of individual taxa using the DESeq2 package, we excluded the rarest taxa by testing only taxa with abundances that were at least 10% of the mean taxon abundance (Wagner *et al.* 2016). This greatly reduced the number of tests to be performed but retained most of the data; for example, across the full dataset it reduced the number of bacterial ASVs from 1502 to 367 while retaining 98.0% of all observations. We explored overall patterns of microbiome variation by performing

multivariate ANOVA on the Bray-Curtis dissimilarity matrix of the full dataset using the function "vegan::adonis" (Oksanen *et al.* 2018). This model included the predictor variables "Genotype", "Rep" (i.e., field and year), "Genotype*Rep", "Timepoint", and "Genotype*Timepoint".

Testing effects of MDR alleles on the juvenile and adult maize microbiomes: Next, we tested the hypothesis that the introgression of MDR alleles altered microbiome composition. We conducted these analyses separately for young plants measured three weeks after planting (the "early" timepoint) and seven weeks after planting (the "late" timepoint). For each timepoint we performed multivariate ANOVA of Bray-Curtis dissimilarity, using a model that included "Genotype", "Rep", and their interaction as predictor variables. Because we were specifically interested in contrasting MDR genotypes to the susceptible line H100 (Figure 2a), we repeated this analysis ten times; each time we subset the data to include only H100 and one other genotype (a MDR NIL or parent line). We took a similar approach to test whether MDR alleles altered alpha diversity and beta diversity. To quantify beta diversity, we used the function "vegan::betadisper" to find a centroid location in ordination space for each Genotype in each Rep, and then to calculate each sample's distance to its corresponding centroid. We then modeled ACE diversity, Shannon diversity, and beta diversity (*i.e.,* distance to centroid) using separate linear mixed-effects models with "Genotype" as a fixed effect and "Rep" as a random-intercept term. The ACE diversity metric was log-transformed to improve homoscedasticity. Standardized sequencing depth and a "Plate" random-intercept term were also included as nuisance variables to control for variation in sampling effort among samples and batch effects during DNA extraction and library preparation. Post-hoc Dunnett *t*-tests (Dunnett 1955) were used to directly contrast each MDR genotype to H100 within each Rep. Finally, to determine which microbial taxa responded to host genotype, we fit negative binomial models to counts of individual ASVs, genera, families, orders, classes, and phyla, using "Genotype", "Rep", and their interaction as predictor variables. For these analyses, H100 was set as the reference genotype, so that the coefficients from the model described contrasts between MDR lines and the disease-susceptible control.

Investigating the effect of disease severity on seasonal microbiome dynamics: To investigate the effect of disease establishment on microbiome succession over time, These analyses used only data from 2017 (Figure 2) and focused on comparison of inoculated fields versus uninoculated fields. Using the function vegan::capscale(), we performed a partial constrained distance-based redundancy analysis (based on the Bray-Curtis dissimilarity metric) to characterize the overall community response to Timepoint*Field interactions after controlling for batch effects. To assess statistical significance of this interaction, we used permutation tests to compare this model to an alternative model containing only the Timepoint and Field main effects. To determine which taxa drove this interaction, we used the DESeq2 package to fit negative binomial models for counts of individual ASVs, genera, families, orders, classes, and phyla in response to the Timepoint*Field interaction; likelihood ratio tests were used to compare these to alternative models with only the Timepoint and Field main effects. To investigate how disease establishment affected alpha and beta diversity at the field level from early season to late season, we calculated each individual plant's change in Shannon diversity and in Distance_to_Centroid between timepoints (centroid calculated for each Field at each Timepoint). We then fit linear mixed models to these calculated values with "Field" as a

fixed-effect predictor. Standardized sequencing depth and a "Plate" random-intercept term were also included as nuisance variables to control for variation in sampling effort and batch effects during DNA extraction and library preparation. Statistical significance was assessed using ANOVA with Type III sums of squares and Satterthwaite's approximation for denominator degrees of freedom, implemented with the R package "lmerTest". We used Tukey's Honest Significant Difference test to compare the early-to-late changes in alpha and beta diversity among fields. Finally, within each of the two inoculated fields, we modeled each plant's change in alpha diversity and in community composition (i.e., Bray-Curtis dissimilarity between the two timepoints) as a function of symptom severity.

Results

TABLE 1 | Results of permutational MANOVA for fungal and bacterial community composition in the leaves of maize plants. *P*-values are based on 999 permutations of the Bray-Curtis dissimilarity matrix calculated from variance-stabilized amplicon sequence variant (ASV) tables.

	Bacteria			**Fungi**		
	R^2	**pseudo-*F* test**	**P**	**R^2**	**pseudo-*F* test**	**P**
Genotype	0.010	$F_{10,1140} = 1.59$	0.001	0.008	$F_{10,1456} = 1.72$	0.001
Timepoint	0.223	$F_{1,1140} = 344.66$	0.001	0.125	$F_{1,1456} = 272.97$	0.001
Rep	0.035	$F_{3,1140} = 18.17$	0.001	0.168	$F_{5,1456} = 73.41$	0.001
Genotype x Timepoint	0.009	$F_{10,1140} = 1.42$	0.003	0.007	$F_{10,1456} = 1.60$	0.001
Genotype x Rep	0.021	$F_{30,1140} = 1.07$	0.198	0.023	$F_{50,1456} = 1.01$	0.436

The final fungal dataset included 548 ASVs and 1,533 samples from 6 replicate plots over two years (2016-2017). The bacterial dataset included 1,502 ASVs and 1,141 samples from 4 replicate plots in 2017 only. The samples from 2017 represented two timepoints: early (3-week-old plants) and late (7-week-old plants), whereas the 2016 data represented the early timepoint only (Figure 2c). At the early timepoint, the median replication was *N*=13 and *N*=14 per genotype per replicate plot for bacteria and fungi, respectively. At the late timepoint, the median replication was *N*=12.5 for bacteria and *N*=11 for fungi. The median sequencing depth per sample was 23,448 for fungi and 97,955 for bacteria.

Bacterial microbiomes were structured largely by timepoint, which explained about 23% of the variation in community composition (Figure 3; PerMANOVA, $P < 0.001$); experimental replicate (i.e., field) and host genotype each explained only about 3% of the variation. At the early timepoint, communities were dominated by *Pantoea* spp. (52.6% relative abundance) followed by *Herbaspirillum* spp. (12.1%). However, four weeks later, the relative abundances of these groups had declined sharply to 4.3% and 2.0%, respectively. The dominant bacterial

members of the adult maize leaf microbiome belonged to the genera *Sphingomonas* (38.4%) and *Methylobacterium* (28.8%; Table S3).

In contrast, fungal communities were shaped most strongly by experimental replicate (i.e., field and year; Table 1); however, timepoint became the dominant predictor when the reps from 2016 were excluded, indicating that differences between years contributed to this result (Figure S3). Excluding sequences that could not be identified, in 2016 the most abundant fungal genus in the leaves of young plants was *Sporobolomyces* (31.7% relative abundance) followed by *Epicoccum* (12.7%). The following year, the same genera were again the two most common in young leaves, although in the opposite order (*Epicoccum* 24.7%, *Sporobolomyces* 8.3%). At the later timepoint, *Epicoccum* remained the most abundant genus in older plants, although its share of the community declined to 9.8% (Table S3).

We detected host genetic effects on overall composition of both bacterial and fungal microbiomes, as well as an interaction between host genotype and timepoint (Table 1); we explore these results in more detail below. On average, alpha diversity of both kingdoms increased between timepoints (Figure 3c-d), *i.e.*, the microbial community within a given leaf sample was more diverse in seven-week-old plants relative to three-week-old plants. In contrast, beta diversity (*i.e.*, variation among samples) of bacterial communities decreased whereas beta diversity of fungal communities increased (Figure 3e-f).

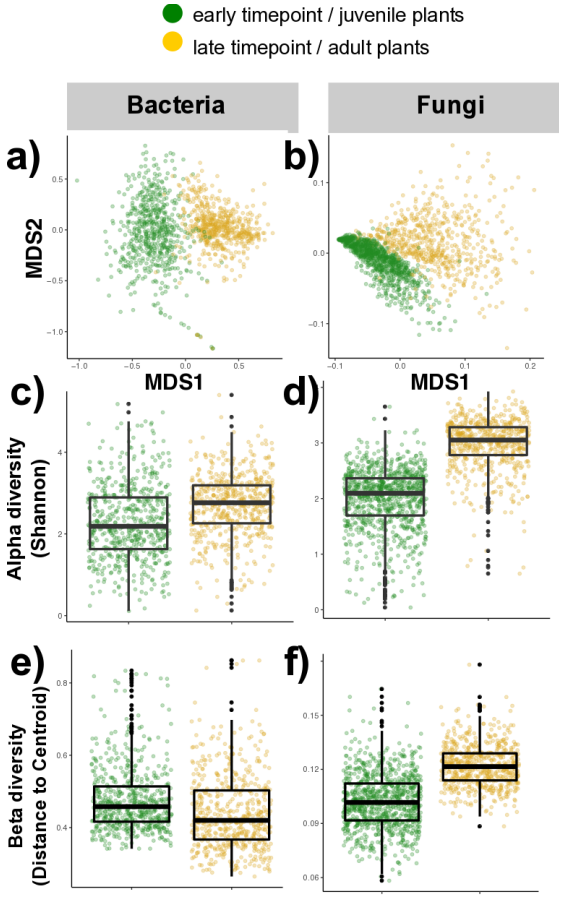

Figure 3 | Maize leaf microbiomes shifted dramatically between 3 weeks and 7 weeks after planting. **(a-b)** Overall microbiome composition shifted strongly between timepoints. MDS1 and MDS2 are the two major

axes of variation after ordination of the Bray-Curtis dissimilarity matrix using non-metric multidimensional scaling, i.e., numerical summaries of community composition. Each point represents one leaf sample; points separated by smaller distances in MDS space indicate samples with more similar microbiomes. **(c-d)** On average, alpha diversity was higher at the late timepoint than the early timepoint. The top, middle, and bottom lines of the boxes mark the 75th percentile, median, and 25th percentile, respectively; box whiskers extend 1.5 times the interquartile range above and below the box. **(e-f)** Beta diversity (*i.e.*, variation among samples) decreased slightly over time for bacteria, but increased for fungi between timepoints. Boxplot statistics are the same as in panels (c-d).

In juvenile plants, MDR alleles altered the composition of the bacterial leaf microbiome

TABLE 2 | Results of permutational MANOVA of fungal and bacterial community composition in maize leaves at two timepoints. Each MDR line was individually compared to the common disease-susceptible genetic background, H100. R^2 values are shown for the Genotype and Genotype*Rep terms of each model. For the early timepoint, the Replicate factor included variation among fields and between years; for the late timepoint, it only included variation among fields. Statistical significance was based on comparison of pseudo-*F* values after 999 permutations of the Bray-Curtis dissimilarity matrix calculated from variance-stabilized ASV tables.

	Bacteria				**Fungi**			
	Early timepoint		**Late timepoint**		**Early timepoint**		**Late timepoint**	
MDR line (vs. H100)	**Geno.**	**Geno. x Rep**	**Geno.**	**Geno. x Rep**	**Geno.**	**Geno. x Rep**	**Geno.**	**Geno. x Rep**
Ki3	**0.012** *	0.020	**0.020****	0.023	0.004	0.016	0.009‡	**0.024** *
DRIL32.063	0.008	0.017	0.015‡	0.026	0.005	0.022	**0.012** *	0.018
DRIL32.095	**0.013** *	0.022	0.007	0.019	0.004	0.017	0.006	0.020
DRIL32.134	**0.013** *	0.014	0.007	0.019	0.004	0.018	**0.012** *	0.020
DRIL32.140	0.005	0.017	0.008	0.021	0.002	0.016	0.008	0.015
DRIL62.030	0.008	0.026	0.016‡	0.034	0.006	0.022	**0.019** **	0.022
DRIL62.032	0.008	0.023	0.011	0.029	0.004	0.018	0.009‡	**0.026** *
DRIL62.054	**0.013** *	0.021	0.008	0.025	0.005	0.018	0.008	0.022
DRIL62.127	0.008	0.016	0.007	0.032	0.002	0.015	0.008	0.019
NC304	**0.013** *	0.027	**0.026****	0.029	0.008	0.023	**0.021** **	**0.030** **

‡FDR<0.1, *FDR<0.05, **FDR<0.01

First, we investigated whether the introgression of MDR alleles altered microbiome composition in the leaves of young maize plants, before the establishment of disease. For these analyses we used data from both years, but included only the data from the early timepoint (3 weeks after planting). We found evidence of genetic variation for alpha diversity of both bacterial and fungal leaf microbiomes, measured using the ACE metric (ANOVA, Genotype x Rep, P = 0.070 and P = 0.0038 respectively; Table S4). However, both the strength and the direction of this effect varied across experimental replicates. In some replicates, the MDR NILs deviated from H100 in the same direction as the MDR parent lines, consistent with the hypothesis that the introgressed QTL alleles affect both disease resistance and early microbiome diversity. In others, however, there was no apparent genetic variation at all (Figure S4). In contrast, we found no evidence that genetic variation influences alpha diversity measured using the Shannon metric (ANOVA, P > 0.05). These results indicate that host genotype interacts with environment in complex ways to influence the richness--but not evenness--of leaf-associated microbiomes in maize. Tests of beta diversity--*i.e*., variation in microbiome composition among individuals of the same genotype in the same experimental replicate--showed similar patterns. We detected genetic variation for beta diversity in both fungal and bacterial communities of juvenile maize leaves, but the direction and strength of the effect were inconsistent among experimental replicates, which incorporate differences between years (for fungi only) and among fields (for bacteria and fungi) (Table S5; Figure S5).

In addition to alpha and beta diversity, we investigated the effects of MDR allele introgression on overall community composition using permutational MANOVA. In addition to the two disease-resistant parent lines used as donors of the introgressed loci, three of the eight NILs differed significantly from H100 in bacterial microbiome composition, suggesting that the alleles introgressed into these lines may play a role in early microbiome assembly (Table 2). In contrast, overall fungal community structure did not differ significantly between any of the MDR lines and H100, contradicting our hypothesis that these MDR loci would have stronger and more consistent effects on fungi than bacteria. Nevertheless, we detected a diverse range of individual taxa that changed in relative abundance in response to MDR allele introgression. For instance, 20 fungal genera were either enriched or depleted in at least one NIL relative to the common disease-susceptible parent line H100, with effect sizes ranging from approximately 4-fold to over 1000-fold (Wald test, FDR < 0.05; Figure 4b). Many of these taxa responded similarly to several non-overlapping introgressions (Figure S1). For example, *Aureobasidium* was depleted in six of the eight NILs, while several other groups including *Selenophoma*, *Moesziomyces*, *Curvularia*, *Mycosphaerella*, *Pseudopithomyces, Pseudozyma*, Kineosporiaceae, Oxalobacteraceae, Caulobacteraceae, and Xanthomonadaceae were all either enriched or depleted consistently across at least three NILs (Figure 4). This strengthens the evidence that broad-spectrum disease resistance and microbiome composition share a genetic basis, because multiple non-overlapping MDR QTL had similar effects on these taxa. However, the inconsistency of the microbiome response across fields and years suggests that these QTL have lower penetrance for microbiome composition than for disease resistance (Lopez-Zuniga *et al.* 2019).

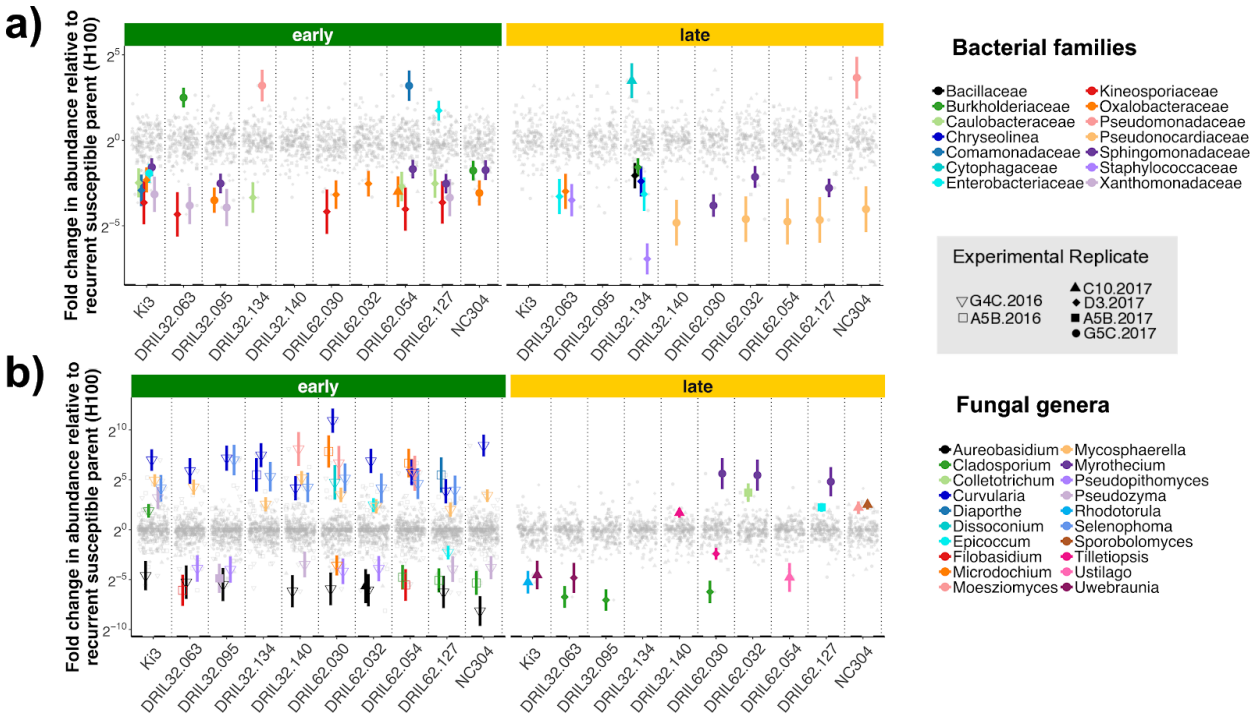

Figure 4 | Introgression of MDR QTL alleles altered the relative abundance of diverse bacterial and fungal taxa in leaves of 3-week-old and 7-week-old maize. Panels **(a)** and **(b)** show the enrichment/depletion of bacterial families and fungal genera (respectively) caused by introgression of MDR alleles into the H100 genetic background (Figure 2). Host genotypes “Ki3” and “NC304” are the MDR parent lines; the others are NILs derived from crosses between those lines and the disease-susceptible line H100 (Figure 2). Taxa with significant changes in relative abundance (Wald test, FDR < 0.05) are shown as colored, enlarged points against the background of all taxa tested (small grey points). Shape indicates the experimental replicate in which the change in relative abundance was observed. Taxa unidentified at the genus level were excluded for clarity.

Sensitivity of the adult maize microbiome to MDR alleles

Second, we investigated whether MDR alleles affected the maize leaf microbiome later in the season, seven weeks after planting. For these analyses we used data from the 2017 experiment only. One week after the first microbiome sampling, plants in two of the four fields received pathogen inoculations so that at the 7-week timepoint plants in field C10 were infected with southern leaf blight and those in field D3 were infected with northern leaf blight. We scored disease symptoms two weeks after inoculation and confirmed that resistance to both diseases was improved in all eight MDR NILs relative to the susceptible parent line H100 (Figure 5; all $P < 4.7e^{-7}$, all $R^2 > 0.70$). However, we collected microbiome data only from green tissue, avoiding lesions of infected plants. ASVs corresponding to the introduced pathogens (*Bipolaris maydis* and *Setosphaeria turcica*) were removed from the dataset before analysis. We took this approach because we were primarily interested in direct effects of MDR alleles on the non-pathogenic microbiome, rather than cascading effects on the microbiome driven by improved disease resistance.

Our results provided mixed support for our hypothesis that host genotype effects would be stronger at the late timepoint than the early timepoint. For example, MDR alleles shaped fungal community structure more strongly in the late timepoint relative to the early timepoint, but the opposite was true for bacteria (Table 2). For both kingdoms, genetic differences in alpha diversity were comparable between timepoints (Figure S4); however, MDR alleles tended to decrease beta diversity of fungal communities only at the later timepoint, and only in the two fields that had been inoculated with pathogens. This suggests that at least some of their effects on the microbiome were mediated through their effects on disease resistance (Figure S5). We detected similar numbers of host-genotype-sensitive bacterial taxa at both timepoints (Figure 4a), whereas changes in relative abundance for fungal taxa were more common at the late timepoint (considering only the 2017 replicates, since no data were available from the late timepoint in 2016; Figure 4b). Additionally, the magnitudes of taxon enrichments and depletions due to MDR allele introgression were comparable between timepoints (Figure 4). There was little overlap between the sets of taxa responding to MDR breeding at the early and late timepoints, with the exceptions of *Cladosporium* and the Sphingomonadaceae, which had lower relative abundance in several MDR lines at both timepoints. This indicates that MDR-induced microbiome differences in seedlings did not generally persist throughout the growing season.

Altogether, our results indicate that introgression of MDR alleles did affect the leaf microbiome composition of both 3-week-old and 7-week-old maize plants by shifting relative abundance of diverse bacterial and fungal taxa (Figure 4). However, the effects of these MDR loci on the microbiome were much more variable among environments than their effects on disease resistance (Lopez-Zuniga *et al.* 2019). This suggests that changes in the relative abundance of potentially protective microbes is unlikely to be a major mechanism by which these particular MDR alleles confer improved disease resistance.

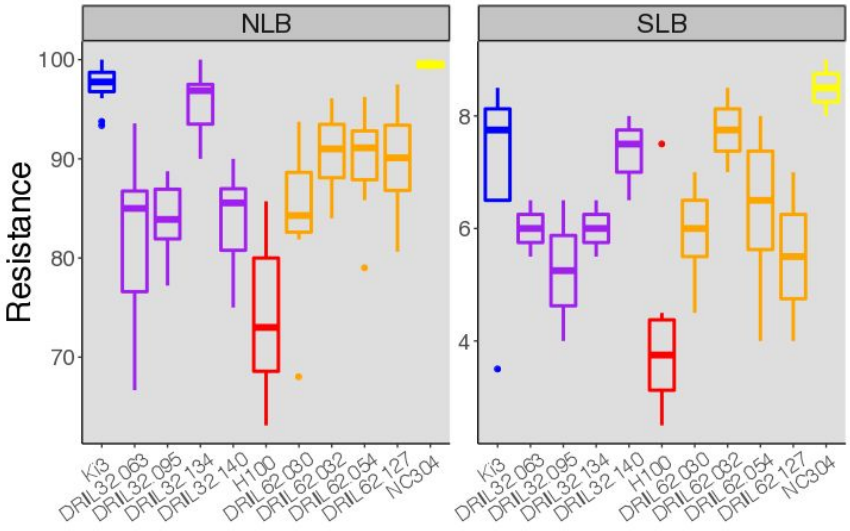

Figure 5 | Introgression of QTL alleles from two MDR parent lines improved resistance to northern leaf blight (NLB; left) and southern leaf blight (SLB; right) in six-week-old plants. Symptoms were scored two weeks after pathogen inoculation. The top, middle, and bottom lines of the boxes mark the 75th percentile, median, and 25th percentile, respectively; box whiskers extend 1.5 times the interquartile range above and below the box. For NLB, all comparisons to the susceptible genetic background H100

were significant at $P < 9.3e^{-4}$ ($N = 141$; genotype $R^2=0.71$); for SLB, all comparisons were significant at $P < 1.6e^{-7}$ ($N = 147$; genotype $R^2=0.76$).

Seasonal microbiome dynamics were largely insensitive to disease status

Finally, we shifted our focus away from host genotype to investigate the relationship between disease and the microbiome more closely. We hypothesized that heavy pathogen infection and disease establishment would disrupt the normal succession of maize leaf microbiomes both (1) at the whole-field level and (2) at the individual plant level. To test these hypotheses, we compared patterns of microbiome change over time in two pathogen-infected fields versus two uninfected control fields, and in heavily-infected individual plants versus less-infected individuals of the same genotype within a field.

Microbiome composition and diversity of all fields changed dramatically between three weeks and seven weeks after planting, regardless of infection status (Figure 6). Community composition diverged among fields over time, although this pattern was much more pronounced for fungi than bacteria (Figure 6a; distance-based redundancy analysis, Timepoint*Field $P = 0.001$). Contrary to our expectation, we observed no clear clustering of disease-inoculated fields from control fields at the late timepoint. Similarly, the relative abundances of individual taxa generally changed in the same direction over time in all four fields (Figure 6b). However, there were a few exceptions. For instance, in infected fields the genera *Ralstonia*, *Staphylococcus*, *Gardnerella*, *Dietzia*, and *Mycobacterium* all decreased between timepoints, but increased between timepoints in the control fields. The fungal genera *Rhodotorula, Bullera,* and *Microdochium* showed the opposite pattern. Nevertheless, infected and uninfected fields were mainly distinguished by the magnitude, rather than the direction, of leaf microbiome succession. The average shift in relative abundance between timepoints was stronger in infected fields than in uninfected fields (Figure 6b-c). Similarly, temporal changes in alpha and beta diversity varied in magnitude among fields for both bacteria and fungi (Figure 6d; ANOVA $P < 0.05$ for all); however, these differences did not correspond to disease treatment.

Because our disease treatments had to be applied to entire fields, replication was low and treatment was confounded with other factors such as the species of crops planted in adjacent fields, proximity to roads and trees, and the species of crops planted the previous year (Figure 2; Table S2). As an additional test to circumvent this problem, we investigated whether temporal changes in microbiome composition and diversity were correlated with disease susceptibility within individual plants. We found no evidence that symptom severity altered microbiome succession in either NLB-infected or SLB-infected plants (linear regression, $P > 0.05$ for both; $N = 115$ or $N = 118$, respectively; Figure S6). This result suggests that overall infection severity at the whole-plant level does not necessarily alter microbiome composition in the remaining green leaf tissue.

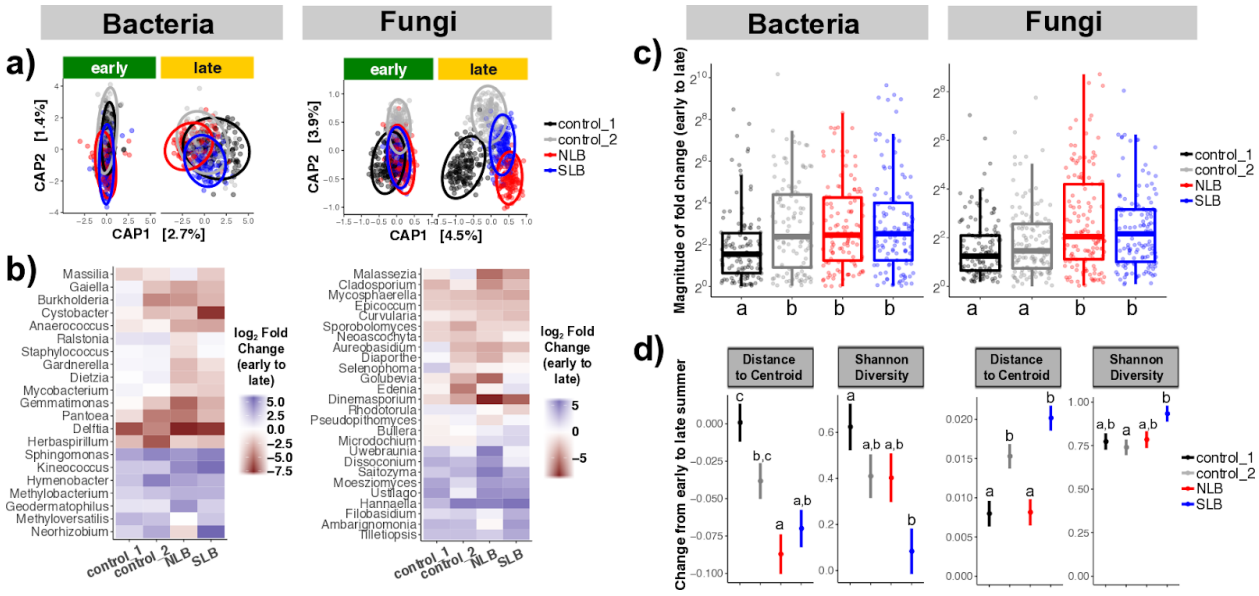

Figure 6 | Maize leaf microbiomes changed over the growing season regardless of disease pressure. All results are shown for four fields that are labeled according to the disease treatment they received (NLB/northern leaf blight, SLB/southern leaf blight, or none/control). **(a)** Partial distance-based redundancy analysis, constrained on the interaction between timepoint and field, shows that microbial communities in different fields became more distinct from each other over time. **(b)** Changes in relative abundance over time varied among fields for all taxa shown (likelihood ratio tests of negative binomial models with and without Timepoint*Field interaction term; FDR < 0.05). **(c)** The average magnitude of fold changes in relative abundance over time varied among fields (ANOVA, $P < 0.001$ for both bacteria and fungi; post-hoc Tukey tests, $P < 0.05$). The top, middle, and bottom lines of the boxes mark the 75th percentile, median, and 25th percentile, respectively; box whiskers extend 1.5 times the interquartile range above and below the box. **(d)** Changes in alpha diversity (Shannon metric) and beta diversity (Distance to centroid) between timepoints differed among fields (ANOVA, all $P < 0.05$; post-hoc Tukey tests, $P < 0.05$).

Discussion

The process of breeding for broad-spectrum disease resistance involves selecting alleles with the ability to alter the invasion success of several different pathogens. We demonstrated that different maize genotypes, identical except for the presence of MDR alleles, assemble different leaf microbial communities both early in development and later in the growing season (Figure 4; Figure S5; Table 1). This shift in community composition involved a wide variety of microbial taxa, likely including both non-pathogenic organisms and potential pathogens. Interestingly, many taxa (*e.g.*, Xanthomonadaceae, *Pseudozyma*, *Aureobasidium*, *Selenophoma*) responded similarly to multiple independent introgressions (Figure 4a-b), suggesting that the underlying genes may involve partially redundant mechanisms. Counterintuitively, seedlings of MDR genotypes were consistently enriched in two fungal genera known to contain many plant pathogens (*Curvularia* and *Mycosphaerella*; Figure 4a), although all plants were asymptomatic at the early timepoint.

Different methods of testing for host genetic effects on the microbiome sometimes led to incongruent conclusions; for example, negative binomial models of individual fungal taxa found stronger genetic effects at the early timepoint than at the late timepoint, while permutational MANOVA found the opposite pattern (Figure 4b; Table 2). However, these outcomes are not necessarily contradictory because the latter method can detect simultaneous shifts in a large number of species, even if most or all of those shifts are too subtle to be detected using univariate models (Anderson 2001). Similarly, strong responses by a small number of taxa may be missed by permutational MANOVA if the rest of the community stays relatively stable.

Our results are consistent with our hypothesis that some MDR loci work through general anti-microbial mechanisms, and therefore also affect non-pathogenic bacteria and fungi. However, because these NILs carried introgressions covering up to 10% of the genome, we cannot rule out the possibility that linked genes--rather than the MDR alleles themselves--caused the observed shifts in microbiome composition. Follow-up experiments comparing these NILs to others with similar-sized introgressions but no MDR improvement would help to disentangle these possibilities. To determine the causal genes for both the MDR phenotype and the associated microbiome changes, further refinement of these lines, additional genetic mapping, and molecular verification would be needed. Nevertheless, our results demonstrate that the introgression of certain MDR alleles can have side-effects on the microbiome. Whether caused by linkage or true pleiotropy, these side-effects have potential to either facilitate or interfere with the process of breeding for increased MDR (Figure 1b).

It is worth noting that our experiment included only four NILs derived from each MDR parent line; combined, these sets of NILs represented no more than 40% of the MDR parent genome (Lopez-Zuniga *et al.* 2019). The inclusion of more NILs from these crosses, which contain MDR alleles at different QTL, would likely have revealed additional MDR-driven microbiome changes. Follow-up work exploring the prevalence of these effects across a wider range of MDR and MDS accessions, including those in other crop and non-crop plant species, would help to determine whether the shared genetic basis of MDR and microbiome composition is broadly generalizable.

We also hypothesized that in addition to direct effects on the microbiome, MDR alleles would also indirectly influence the microbiome through cascading effects of differences in infection severity (Figure 1a). As a result, we expected to observe stronger host genotype effects after disease establishment. However, our data only partially supported this hypothesis, which relied on the assumption that disease establishment would profoundly disrupt the microbiome, as has been described in soil (Chapelle *et al.* 2016). However, comparisons of microbiome composition in infected versus uninfected fields, and of severely versus mildly infected plants, did not consistently support this assumption (Figure 6; Figure S6). We propose several possible explanations for the weaker-than-expected effect of pathogen invasion on the maize leaf microbiome. First, we deliberately sampled green tissue and avoided lesions (Figure S2), which likely biased our dataset away from capturing the most strongly perturbed local communities. This choice was intentional because our primary interest was in direct effects of MDR alleles on non-pathogenic microbes; nevertheless, we expected to observe changes in microbiome composition as a result of the plant's systemic response to infection (Gu *et al.* 2016; Hacquard *et al.* 2017). Second, the observed succession between timepoints (Figure 2) likely

reflected many different causal factors, including plant development and strong morphological differences between juvenile and adult leaves, a changing biotic context including insect communities and neighboring plants, and increased temperature and community. The combined impact of these factors on the microbiome may have swamped out any signal of pathogen invasion. Finally, because our disease treatments could only be applied at the whole-field level, differences in microbial succession among fields also could have masked community responses to disease. A follow-up experiment that randomizes disease treatments while minimizing such environmental variation would help to explain this observation.

The partially-shared genetic basis of MDR and microbiome composition suggests that breeding for broad-spectrum disease resistance is likely to have side-effects on colonization by other microbial symbionts. The upshot of these side-effects for plant health--and ultimately, breeding outcomes--depends on whether individual symbionts increase or decrease in frequency due to host genetic improvement, and whether they have a positive or negative effect on the host (Figure 1b). The resolution of the amplicon sequencing approach that we used in this experiment is insufficient to determine what effects the enriched or depleted taxa had on the experimental plants, if any. Re-inoculation experiments under controlled conditions would be necessary to determine whether these organisms affect disease resistance either positively or negatively. Another unresolved question that our data could not address is whether MDR alleles affected leaf microbiomes in ways other than changing relative abundance-- for example, by altering the total microbial load in leaves or by inducing changes in microbial gene expression and metabolic activity, which also could contribute to disease resistance (Chapelle *et al.* 2016). Understanding these complex links between the plant microbiota, pathogens, host phenotype, and environment will be crucial for developing microbiome-based solutions for sustainable disease control (Massart *et al.* 2015; Berg *et al.* 2017; Busby *et al.* 2017).

Acknowledgements:

We thank G. Marshall, J. Roberts, S. Sermons, and J. Torres for assistance with field and lab work, and we thank E. Barge, L. Burghardt, and D. Leopold for valuable comments and feedback on the manuscript. We thank Cathy Herring and the staff at NC Central Crops Research farm for managing the field trials. M.R.W. was supported by a NSF National Plant Genome Initiative Postdoctoral Research Fellowship in Biology (IOS-1612951). P.E.B. was supported by the NSF Science, Engineering, and Education for Sustainability Fellows program (CHE-1314095). This work was funded by a NCSU Plant Soil Microbial Community Consortium grant to P.B.K. and M.R.W.

Supplementary Information

Table S1 | Maize lines used in this experiment. The eight "DRIL" lines were near-isogenic lines descended from crosses between the disease-susceptible inbred line H100 and one of two disease-resistant inbred lines (Ki3 or NC304; Figure 2a). On average, the DRIL lines retained ~6.25% of their genome from the MDR donor line (Lopez-Zuniga et al. 2019).

Line	MDR parent (donor)	MDS parent (recurrent)
H100	---	H100
Ki3	Ki3	---
NC304	NC304	---
DRIL32.063	Ki3	H100
DRIL32.095	Ki3	H100
DRIL32.134	Ki3	H100
DRIL32.140	Ki3	H100
DRIL62.030	NC304	H100
DRIL62.032	NC304	H100
DRIL62.054	NC304	H100
DRIL62.127	NC304	H100

Table S2 | Fields used for this experiment. All were located at Central Crops Research Station in Clayton, North Carolina, USA (Figure 2). No pair of fields was separated by more than 2 km.

Field	Soil type	**Rotation** (2014-2017)	Data collection	Disease Treatment (2017 only)
A5B	Wagram loamy sand	Squash > Soybean > Corn > Corn	2016-2017	Uninoculated control
C10	Dothan loamy sand	Soybean > Corn > Cotton > Corn	2017	SLB
D3	Gilead sandy loam	Wheat/Fava bean > Cotton > Corn/Winter pea > Corn	2017	NLB
G4C	Norfolk loamy sand	Corn > Soybean > Corn > Tobacco	2016	NA
G5C	Wagram loamy sand	Corn > Tobacco > Cucumber > Corn	2017	Uninoculated control

Table S3 | The 20 most abundant genera in leaves of 3-week-old ("early") and 7-week-old ("late") maize plants, with their relative abundances. Parentheses indicate groups that could not be identified at the genus level.

Bacteria				Fungi					
Early (2017)		Late (2017)		Early (2016)		Early (2017)		Late (2017)	
Pantoea	0.526	Sphingomonas	0.384	Sporobolomyces	0.317	(unidentified)	0.367	unidentified	0.267
Herbaspirillum	0.121	Methylobacterium	0.288	(unidentified)	0.174	Epicoccum	0.247	Epicoccum	0.098
Methylobacterium	0.044	Pantoea	0.043	Epicoccum	0.127	Sporobolomyces	0.083	Moesziomyces	0.088
Bacillus	0.032	Bacillus	0.029	Naganishia	0.064	Mycosphaerella	0.060	Tilletiopsis	0.086
Lactobacillus	0.027	Hymenobacter	0.025	Diaporthe	0.056	Cryptococcus	0.035	Hannaella	0.054
Sphingomonas	0.025	Ralstonia	0.022	Rhodotorula	0.038	Cladosporium	0.018	Filobasidium	0.036
Ralstonia	0.022	Lactobacillus	0.021	Tilletiopsis	0.021	Neoascochyta	0.017	Microdochium	0.026
Massilia	0.019	Herbaspirillum	0.020	Cryptococcus	0.020	Microdochium	0.016	Saitozyma	0.025
Pseudomonas	0.016	Pseudomonas	0.015	(Pleosporales)	0.020	Moesziomyces	0.012	Sporobolomyces	0.025
Burkholderia	0.014	Quadrisphaera	0.014	Bullera	0.016	Curvularia	0.012	Dissoconium	0.025
Escherichia	0.013	Geodermatophilus	0.013	Filobasidium	0.014	Tilletiopsis	0.009	Cryptococcus	0.024
Brevundimonas	0.011	Escherichia	0.011	Neoascochyta	0.014	(Pleosporales)	0.008	Pseudozyma	0.022
Salmonella	0.010	Massilia	0.010	Saitozyma	0.013	(Dothideomycetes)	0.008	Bullera	0.021
Staphylococcus	0.009	Curtobacterium	0.008	Sakaguchia	0.012	Pseudozyma	0.008	(Pleosporales)	0.016
Streptococcus	0.008	Salmonella	0.008	Microdochium	0.012	(Stachybotryaceae)	0.008	Mycosphaerella	0.015
Listeria	0.007	Listeria	0.007	Dioszegia	0.010	Bullera	0.007	Selenophoma	0.014
Enterococcus	0.004	Staphylococcus	0.006	Mycosphaerella	0.009	Filobasidium	0.006	Cercospora	0.013
Enterobacter	0.004	Kineococcus	0.004	Cladosporium	0.009	Selenophoma	0.006	Neoascochyta	0.011
Delftia	0.004	Enterococcus	0.004	Moesziomyces	0.009	(Ascomycota)	0.005	Uwebraunia	0.010
Arthrobacter	0.004	Methyloversatilis	0.004	Papiliotrema	0.007	Pseudopithomyces	0.005	(Tremellales)	0.009

Table S4 | Results of ANOVA of alpha diversity (ACE metric) for fungal and bacterial communities in the leaves of **(a)** maize seedlings three weeks after planting, and **(b)** adult maize seven weeks after planting. Linear mixed-effects models were fitted to log-transformed ACE values with predictors Genotype*Replicate while controlling for sequencing depth and batch effects; separate models were fit for the early and late timepoints. Least-squares mean estimates for each MDR genotype (relative to H100) are displayed in Figure S4.

(a) Early timepoint	**Fungi**		**Bacteria**	
	***F* test**	***P***	***F* test**	***P***
Genotype	$F_{10,531} = 1.21$	0.28	$F_{10,477} = 1.47$	0.15
Rep	$F_{5,535} = 25.91$	$2.7e^{-11}$	$F_{3,477} = 6.36$	0.00031
Genotype x Rep	$F_{48,527} = 1.68$	0.0038	$F_{30,476} = 1.43$	0.070
(b) Late timepoint	**Fungi**		**Bacteria**	
	***F* test**	***P***	***F* test**	***P***
Genotype	$F_{10,542} = 1.69$	0.078	$F_{10,495} = 2.63$	0.004
Rep	$F_{3,542} = 2.89$	0.035	$F_{3,496} = 9.02$	$8.0e^{-6}$
Genotype x Rep	$F_{30,542} = 1.32$	0.12	$F_{30,495} = 2.21$	0.0003

Table S5 | Results of ANOVA of beta diversity (distance from centroid) for fungal and bacterial communities in the leaves of **(a)** maize seedlings three weeks after planting, and **(b)** adult maize seven weeks after planting. Linear mixed-effects models were fitted to each individual's distance to centroid, with predictors Genotype*Replicate while controlling for sequencing depth and batch effects; separate models were fit for the early and late timepoints. LS mean estimates for each MDR genotype (relative to H100) are displayed in Figure S5.

(a) Early timepoint	**Fungi**		**Bacteria**	
	***F* test**	**P**	***F* test**	**P**
Genotype	$F_{10,855} = 1.43$	0.16	$F_{10,536} = 1.93$	0.039
Rep	$F_{5,63} = 19.41$	$1.2e^{-11}$	$F_{3,537} = 7.72$	$4.7e^{-5}$
Genotype x Rep	$F_{50,855} = 1.35$	0.057	$F_{30,535} = 1.22$	0.20
(b) Late timepoint	**Fungi**		**Bacteria**	
	***F* test**	**P**	***F* test**	**P**
Genotype	$F_{10,555} = 3.47$	0.0002	$F_{10,508} = 1.56$	0.12
Rep	$F_{3,555} = 4.72$	0.0029	$F_{3,508} = 9.19$	$6.2e^{-6}$
Genotype x Rep	$F_{30,555} = 2.04$	0.0010	$F_{30,508} = 1.79$	0.0067

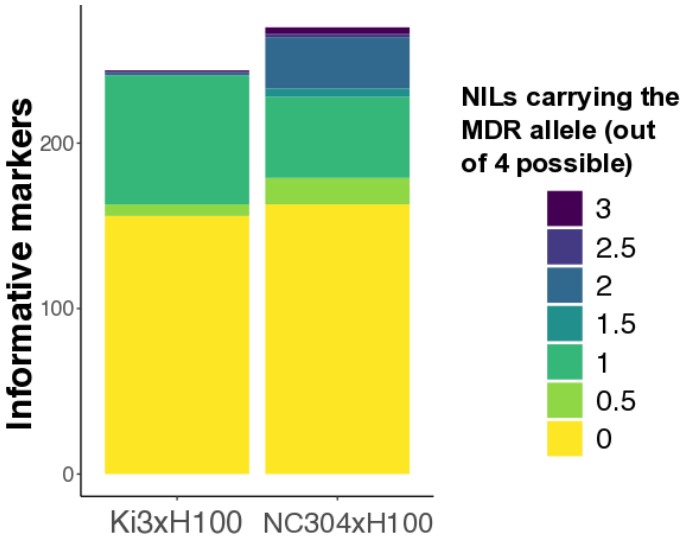

Figure S1 | The introgressed MDR alleles carried by the eight NILs in this study had little overlap. The parent lines and NILs were genotyped using 245 or 270 informative markers (for the Ki3 x H100 cross and the NC304 x H100 cross, respectively). Most alleles from the MDR parent were present in only one NIL or not at all; for both crosses, all four NILs carried the H100 allele for >60% of markers. Observations of MDR alleles in the heterozygous state were scored as 0.5 rather than 1. Data from Lopez-Zuniga et al. (2019).

Figure S2 | For diseased plants, we avoided lesions and targeted green tissue for microbiome analysis.

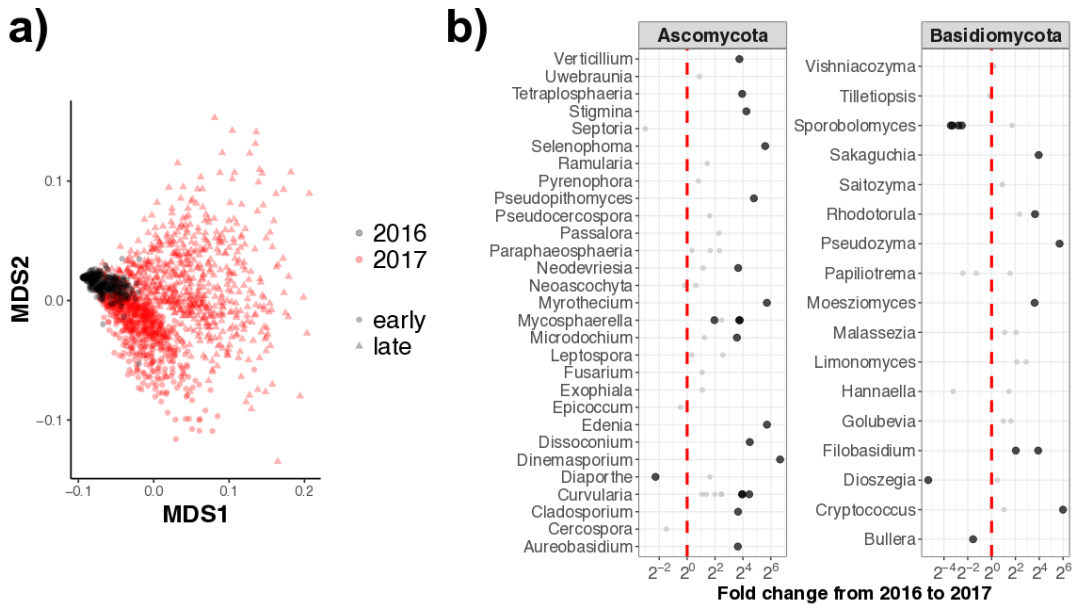

Figure S3 | The foliar fungal microbiome of three-week-old maize seedlings changed between years. **(a)** Non-metric multidimensional scaling of Bray-Curtis dissimilarities reveals that the early-timepoint samples from 2016 (black circles) cluster apart from the early-timepoint samples from 2017 (red circles); however, all early-timepoint samples (black and red circles) cluster apart from late-season samples (red triangles). **(b)** In seedlings growing in “A5B”, the only field that was sampled in both years, many ASVs changed in relative abundance from 2016 to 2017. Grey points represent ASVs that did not change significantly between years; black points represent ASVs that were either more or less abundant in 2017 relative to 2016 (shown to the right or left of the dashed red line, respectively; FDR < 0.05).

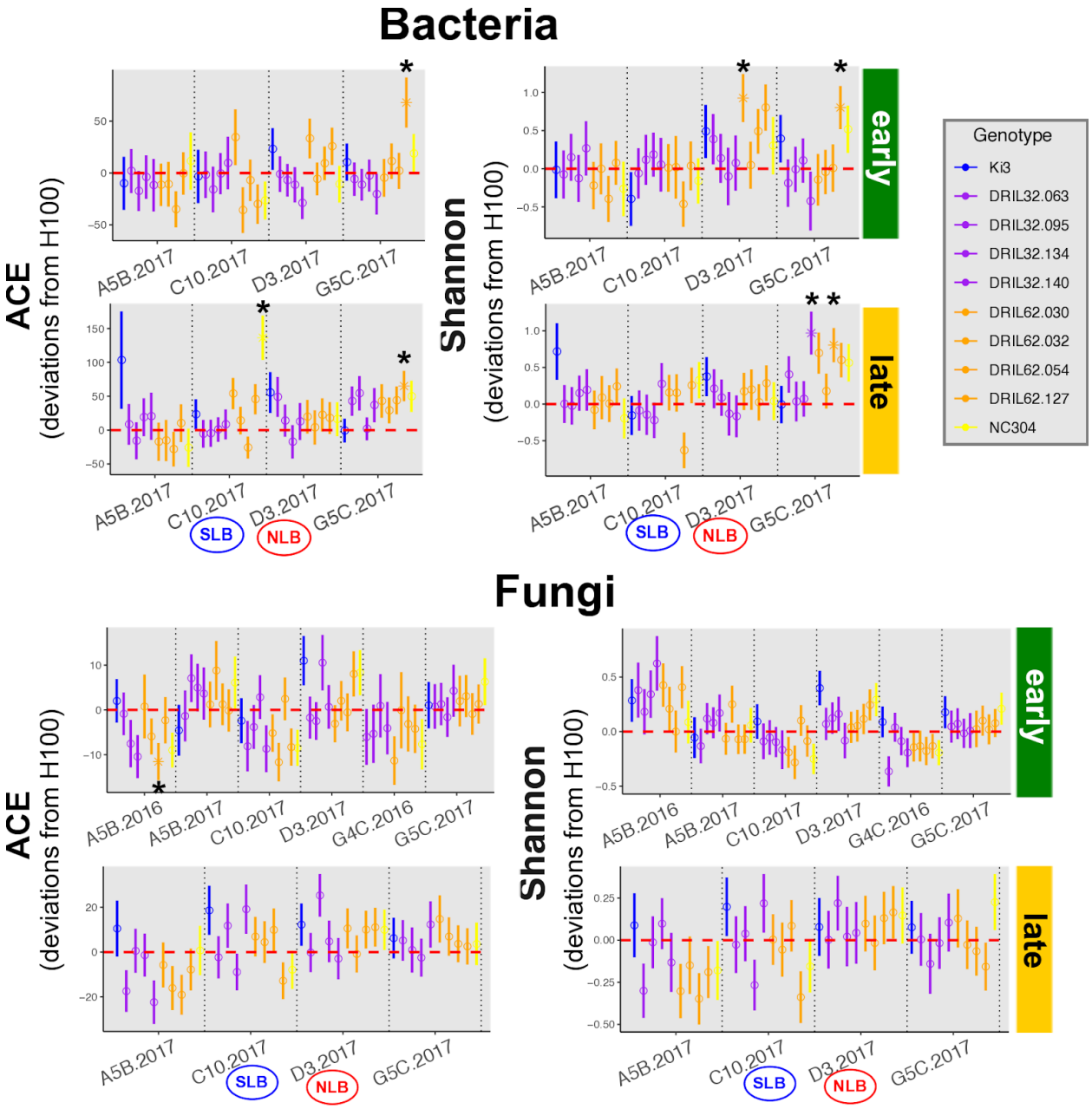

Figure S4 | MDR breeding shaped maize leaf alpha diversity (ACE and Shannon metrics). For each MDR genotype, its estimated deviation from the disease-susceptible line H100 is shown (based on LS means from linear mixed-effects models with predictors Genotype, Replicate, and Genotype*Replicate). Positive values for a given genotype indicate that within-sample diversity was higher than it was for the disease-susceptible line H100; negative values indicate that within-sample diversity was lower relative to H100. Error bars = +/- 1 s.e.m. Open circles mark deviations from H100 that were not significantly different from zero after *P*-value correction using Dunnett's procedure; significant deviations from H100 are shown as asterisks. Corresponding ANOVA results are given in Table S4.

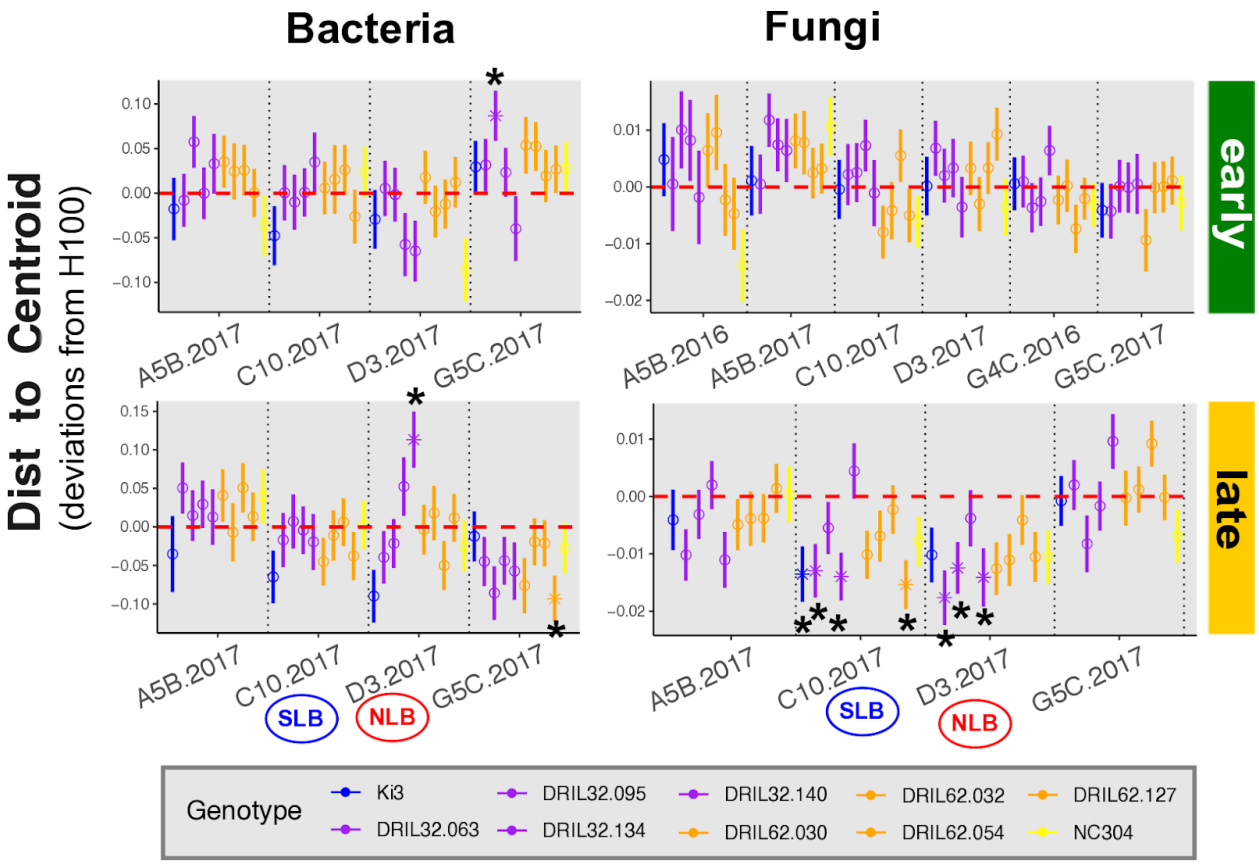

Figure S5 | MDR breeding shaped maize leaf beta diversity (Distance to Centroid). For each MDR genotype, its estimated deviation from the disease-susceptible line H100 is shown (based on LS means from linear mixed-effects models with predictors Genotype, Replicate, and Genotype*Replicate). Positive values indicate that inter-individual variation within a genotype was higher than it was within the disease-susceptible line H100; negative values indicate that inter-individual variation was lower than in H100. Error bars = +/- 1 s.e.m. Open circles mark deviations from H100 that were not significantly different from zero after *P*-value correction using Dunnett's procedure; significant deviations from H100 are shown as asterisks. Corresponding ANOVA results are given in Table S4.

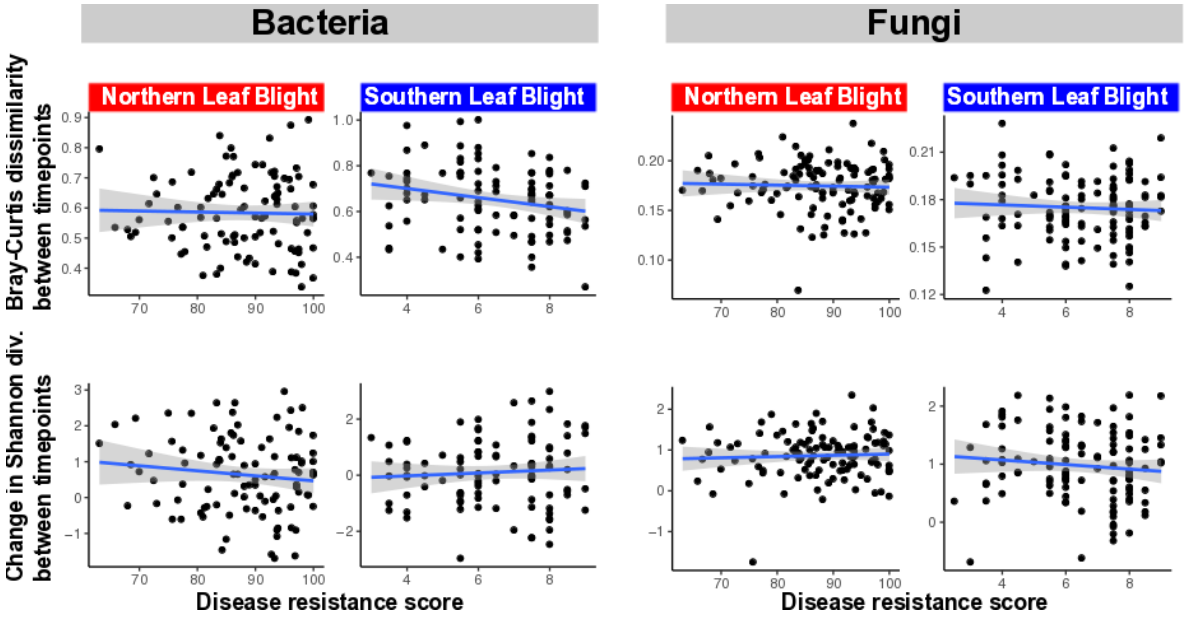

Figure S6 | Within individual plants, temporal changes in community composition (top, quantified as Bray-Curtis dissimilarity between timepoints) and alpha diversity (bottom, quantified as the change in Shannon diversity between timepoints) did not correlate with disease resistance (linear regression, $P > 0.05$ for all tests). For NLB, $N = 115$; for SLB, $N = 118$.

References

Anderson, M.J. (2001). A new method for non-parametric multivariate analysis of variance. *Austral Ecology*.

Bates, D., Mächler, M., Bolker, B. & Walker, S. (2015). Fitting Linear Mixed-Effects Models Usinglme4. *Journal of Statistical Software*.

Beckers, B., Op De Beeck, M., Weyens, N., Van Acker, R., Van Montagu, M., Boerjan, W., *et al.* (2016). Lignin engineering in field-grown poplar trees affects the endosphere bacterial microbiome. *Proc. Natl. Acad. Sci. U. S. A.*, 113, 2312–2317.

Benjamini, Y. & Hochberg, Y. (1995). Controlling the False Discovery Rate: A Practical and Powerful Approach to Multiple Testing. *Journal of the Royal Statistical Society: Series B (Methodological)*.

Berg, G., Köberl, M., Rybakova, D., Müller, H., Grosch, R. & Smalla, K. (2017). Plant microbial diversity is suggested as the key to future biocontrol and health trends. *FEMS Microbiol. Ecol.*, 93.

Berg, M. & Koskella, B. (2018). Nutrient- and Dose-Dependent Microbiome-Mediated Protection against a Plant Pathogen. *Current Biology*.

Bessire, M., Chassot, C., Jacquat, A.-C., Humphry, M., Borel, S., Petétot, J.M.-C., *et al.* (2007). A permeable cuticle in Arabidopsis leads to a strong resistance to Botrytis cinerea. *EMBO J.*, 26, 2158–2168.

Bodenhausen, N., Bortfeld-Miller, M., Ackermann, M. & Vorholt, J.A. (2014). A synthetic community approach reveals plant genotypes affecting the phyllosphere microbiota. *PLoS Genet.*, 10, e1004283.

Bressan, M., Roncato, M.-A., Bellvert, F., Comte, G., Haichar, F.Z., Achouak, W., *et al.* (2009). Exogenous glucosinolate produced by Arabidopsis thaliana has an impact on microbes in the rhizosphere and plant roots. *ISME J.*, 3, 1243–1257.

Bringel, F. & Couée, I. (2015). Pivotal roles of phyllosphere microorganisms at the interface between plant functioning and atmospheric trace gas dynamics. *Front. Microbiol.*, 6, 486.

Brown, B. (2019). *microfiltR: marker gene processing, filtering and exporting functions*.

Busby, P.E., Peay, K.G. & Newcombe, G. (2016). Common foliar fungi of Populus trichocarpa modify Melampsora rust disease severity. *New Phytol.*, 209, 1681–1692.

Busby, P.E., Soman, C., Wagner, M.R., Friesen, M.L., Kremer, J., Bennett, A., *et al.* (2017). Research priorities for harnessing plant microbiomes in sustainable agriculture. *PLoS Biol.*, 15, e2001793.

Callahan, B.J., McMurdie, P.J., Rosen, M.J., Han, A.W., Johnson, A.J.A. & Holmes, S.P. (2016). DADA2: High-resolution sample inference from Illumina amplicon data. *Nat. Methods*, 13, 581–583.

Chapelle, E., Mendes, R., Bakker, P.A.H.M. & Raaijmakers, J.M. (2016). Fungal invasion of the rhizosphere microbiome. *ISME J.*, 10, 265–268.

Clay, K. (1990). Fungal Endophytes Of Grasses. *Annual Review of Ecology and Systematics*.

Cole, J.R., Wang, Q., Fish, J.A., Chai, B., McGarrell, D.M., Sun, Y., *et al.* (2014). Ribosomal Database Project: data and tools for high throughput rRNA analysis. *Nucleic Acids Res.*, 42, D633–42.

Dunnett, C.W. (1955). A Multiple Comparison Procedure for Comparing Several Treatments with a Control. *Journal of the American Statistical Association*.

Fürnkranz, M., Wanek, W., Richter, A., Abell, G., Rasche, F. & Sessitsch, A. (2008). Nitrogen fixation by phyllosphere bacteria associated with higher plants and their colonizing epiphytes of a tropical lowland rainforest of Costa Rica. *ISME J.*, 2, 561–570.

Gu, Y., Wei, Z., Wang, X., Friman, V.-P., Huang, J., Wang, X., *et al.* (2016). Pathogen invasion indirectly changes the composition of soil microbiome via shifts in root exudation profile. *Biology and Fertility of Soils*.

Hacquard, S., Spaepen, S., Garrido-Oter, R. & Schulze-Lefert, P. (2017). Interplay Between Innate Immunity and the Plant Microbiota. *Annu. Rev. Phytopathol.*, 55, 565–589.

Horton, M.W., Bodenhausen, N., Beilsmith, K., Meng, D., Muegge, B.D., Subramanian, S., *et al.* (2014). Genome-wide association study of Arabidopsis thaliana leaf microbial community. *Nat. Commun.*, 5, 5320.

Hughes, J.B., Hellmann, J.J., Ricketts, T.H. & Bohannan, B.J. (2001). Counting the uncountable: statistical approaches to estimating microbial diversity. *Appl. Environ. Microbiol.*, 67, 4399–4406.

Humphrey, P.T., Nguyen, T.T., Villalobos, M.M. & Whiteman, N.K. (2014). Diversity and abundance of phyllosphere bacteria are linked to insect herbivory. *Mol. Ecol.*, 23, 1497–1515.

Kachroo, A. & Kachroo, P. (2009). Fatty Acid-derived signals in plant defense. *Annu. Rev. Phytopathol.*, 47, 153–176.

Kõljalg, U., Larsson, K.-H., Abarenkov, K., Nilsson, R.H., Alexander, I.J., Eberhardt, U., *et al.* (2005). UNITE: a database providing web-based methods for the molecular identification of ectomycorrhizal fungi. *New Phytol.*, 166, 1063–1068.

Krattinger, S.G., Lagudah, E.S., Spielmeyer, W., Singh, R.P., Huerta-Espino, J., McFadden, H., *et al.* (2009). A putative ABC transporter confers durable resistance to multiple fungal pathogens in wheat. *Science*, 323, 1360–1363.

Kuznetsova, A., Brockhoff, P.B. & Christensen, R.H.B. (2017). lmerTest Package: Tests in Linear Mixed Effects Models. *Journal of Statistical Software*.

Laforest-Lapointe, I., Paquette, A., Messier, C. & Kembel, S.W. (2017). Leaf bacterial diversity mediates plant diversity and ecosystem function relationships. *Nature*, 546, 145–147.

Lebeis, S.L., Paredes, S.H., Lundberg, D.S., Breakfield, N., Gehring, J., McDonald, M., *et al.* (2015). PLANT MICROBIOME. Salicylic acid modulates colonization of the root microbiome by specific bacterial taxa. *Science*, 349, 860–864.

Lindow, S.E. & Brandl, M.T. (2003). Microbiology of the phyllosphere. *Appl. Environ. Microbiol.*, 69, 1875–1883.

Loake, G. & Grant, M. (2007). Salicylic acid in plant defence—the players and protagonists. *Current Opinion in Plant Biology*.

Lopez-Zuniga, L.O., Wolters, P., Davis, S., Weldekidan, T., Kolkman, J.M., Nelson, R., *et al.* (2019). Using Maize Chromosome Segment Substitution Line Populations for the Identification of Loci Associated with Multiple Disease Resistance. *G3* , 9, 189–201.

Love, M.I., Huber, W. & Anders, S. (2014). Moderated estimation of fold change and dispersion for RNA-seq data with DESeq2. *Genome Biol.*, 15, 550.

Lundberg, D.S., Lebeis, S.L., Paredes, S.H., Yourstone, S., Gehring, J., Malfatti, S., *et al.* (2012). Defining the core Arabidopsis thaliana root microbiome. *Nature*, 488, 86–90.

Lundberg, D.S., Yourstone, S., Mieczkowski, P., Jones, C.D. & Dangl, J.L. (2013). Practical innovations for high-throughput amplicon sequencing. *Nat. Methods*, 10, 999–1002.

Maignien, L., DeForce, E.A., Chafee, M.E., Eren, A.M. & Simmons, S.L. (2014). Ecological succession and stochastic variation in the assembly of Arabidopsis thaliana phyllosphere communities. *MBio*, 5, e00682–13.

Martin, J.T. (1964). Role of Cuticle in the Defense against Plant Disease. *Annual Review of Phytopathology*.

Martin, M. (2011). Cutadapt removes adapter sequences from high-throughput sequencing reads. *EMBnet.journal*.

Massart, S., Martinez-Medina, M. & Haissam Jijakli, M. (2015). Biological control in the microbiome era: Challenges and opportunities. *Biological Control*.

McMurdie, P.J. & Holmes, S. (2013). phyloseq: An R Package for Reproducible Interactive Analysis and Graphics of Microbiome Census Data. *PLoS ONE*.

McMurdie, P.J. & Holmes, S. (2014). Waste not, want not: why rarefying microbiome data is inadmissible. *PLoS Comput. Biol.*, 10, e1003531.

Murty, M.G. (1984). Phyllosphere of cotton as a habitat for diazotrophic microorganisms. *Appl. Environ. Microbiol.*, 48, 713–718.

Niks, R.E., Qi, X. & Marcel, T.C. (2015). Quantitative Resistance to Biotrophic Filamentous Plant Pathogens: Concepts, Misconceptions, and Mechanisms. *Annual Review of Phytopathology*.

Oksanen, J., Blanchet, F.G., Friendly, M., Kindt, R., Legendre, P., McGlinn, D., *et al.* (2018). *vegan: Community Ecology Package*.

Papen, H., Gessler, A., Zumbusch, E. & Rennenberg, H. (2002). Chemolithoautotrophic nitrifiers in the phyllosphere of a spruce ecosystem receiving high atmospheric nitrogen input. *Curr. Microbiol.*, 44, 56–60.

Poland, J.A., Balint-Kurti, P.J., Wisser, R.J., Pratt, R.C. & Nelson, R.J. (2009). Shades of gray: the world of quantitative disease resistance. *Trends Plant Sci.*, 14, 21–29.

Rife, T.W. & Poland, J.A. (2014). Field Book: An Open-Source Application for Field Data Collection on Android. *Crop Science*.

Ritpitakphong, U., Falquet, L., Vimoltust, A., Berger, A., Métraux, J.-P. & L'Haridon, F. (2016). The microbiome of the leaf surface of Arabidopsis protects against a fungal pathogen. *New Phytol.*, 210, 1033–1043.

Rodriguez, R.J., White, J.F., Jr, Arnold, A.E. & Redman, R.S. (2009). Fungal endophytes: diversity and functional roles. *New Phytol.*, 182, 314–330.

Sapkota, R., Knorr, K., Jørgensen, L.N., O'Hanlon, K.A. & Nicolaisen, M. (2015). Host genotype is an important determinant of the cereal phyllosphere mycobiome. *New Phytol.*, 207, 1134–1144.

Schardl, C.L., Leuchtmann, A. & Spiering, M.J. (2004). Symbioses of grasses with seedborne fungal endophytes. *Annu. Rev. Plant Biol.*, 55, 315–340.

Schnippenkoetter, W., Lo, C., Liu, G., Dibley, K., Chan, W.L., White, J., *et al.* (2017). The wheat Lr34 multipathogen resistance gene confers resistance to anthracnose and rust in sorghum. *Plant Biotechnol. J.*, 15, 1387–1396.

Sermons, S. & Balint-Kurti, P. (2018). Large Scale Field Inoculation and Scoring of Maize Southern Leaf Blight and Other Maize Foliar Fungal Diseases. *BIO-PROTOCOL*.

Serrano, M., Coluccia, F., Torres, M., L'Haridon, F. & Métraux, J.-P. (2014). The cuticle and plant defense to pathogens. *Front. Plant Sci.*, 5, 274.

St Clair, D.A. (2010). Quantitative disease resistance and quantitative resistance Loci in breeding. *Annu. Rev. Phytopathol.*, 48, 247–268.

Sucher, J., Boni, R., Yang, P., Rogowsky, P., Büchner, H., Kastner, C., *et al.* (2017). The durable wheat disease resistance gene Lr34 confers common rust and northern corn leaf blight resistance in maize. *Plant Biotechnol. J.*, 15, 489–496.

Vorholt, J.A. (2012). Microbial life in the phyllosphere. *Nat. Rev. Microbiol.*, 10, 828–840.

Wagner, M.R., Lundberg, D.S., Del Rio, T.G., Tringe, S.G., Dangl, J.L. & Mitchell-Olds, T. (2016). Host genotype and age shape the leaf and root microbiomes of a wild perennial plant. *Nat. Commun.*, 7, 12151.

Wallace, J.G., Kremling, K.A., Kovar, L.L. & Buckler, E.S. (2018). Quantitative Genetics of the Maize Leaf Microbiome. *Phytobiomes Journal*.

Wang, Q., Garrity, G.M., Tiedje, J.M. & Cole, J.R. (2007). Naive Bayesian classifier for rapid assignment of rRNA sequences into the new bacterial taxonomy. *Appl. Environ. Microbiol.*, 73, 5261–5267.

Wiesner-Hanks, T. & Nelson, R. (2016). Multiple Disease Resistance in Plants. *Annu. Rev. Phytopathol.*, 54, 229–252.

Wisser, R.J., Kolkman, J.M., Patzoldt, M.E., Holland, J.B., Yu, J., Krakowsky, M., *et al.* (2011). Multivariate analysis of maize disease resistances suggests a pleiotropic genetic basis and implicates a GST gene. *Proceedings of the National Academy of Sciences*.

Yang, Q., Balint-Kurti, P. & Xu, M. (2017). Quantitative Disease Resistance: Dissection and Adoption in Maize. *Molecular Plant*.

Lindow, S.E. & Brandl, M.T. (2003). Microbiology of the phyllosphere. *Applied and Environmental Microbiology*, 69, 1875–1883.